

Soft QCD Physics at the LHC: highlights and opportunities

P. Christiansen,¹ and P. Van Mechelen²

¹Department of Physics, Lund University, Lund, Sweden, SE-22362; email: peter.christiansen@fysik.lu.se

²Department of Physics, Antwerp University, Antwerp, Belgium, B-2020; email: pierre.vanmechelen@uantwerpen.be

Xxxx. Xxx. Xxx. Xxx. YYYY. AA:1–25

<https://doi.org/10.1146/annurev-nucl-121423-101050>

Copyright © YYYY by the author(s).
All rights reserved

Keywords

LHC, pp collisions, soft QCD, underlying event, quark-gluon plasma

Abstract

The Large Hadron Collider (LHC) at CERN in Switzerland became operational in 2009 and has since then produced a plethora of results for proton-proton (pp) collisions. This short review covers results that relates to soft QCD focusing on non-diffractive physics at mid-rapidity. Most of the presented results comes from transverse momentum (p_T) spectra and related/derived observables such as multiplicity, $\langle p_T \rangle$ and ratios, but also the observed “ridge” and the questions of quark-gluon plasma in pp collisions will be discussed. The goal of the review is on one hand to introduce the topics and provide references for scientists joining the LHC program while at the same time highlighting what we consider the most interesting results and open questions to inspire novel measurements.

Contents

1. Introduction	2
2. A Brief Historical Introduction	3
3. Phenomenological Modeling Perspectives	6
3.1. Multiple-Parton Interactions	7
3.2. Intrinsic transverse momentum and initial and final state radiation	7
3.3. Hadronization and color reconnection	8
3.4. Summary of Generators	9
4. Multiparton Interactions and Underlying Event Tunes	10
4.1. Underlying Event Observables	10
4.2. Monte Carlo Tunes	11
4.3. Tune validation	11
5. Particle Production of identified particles	13
5.1. Lessons from hard production	14
5.2. Review of identified particle spectra and production rates	14
5.3. Baryon production	17
6. Collectivity: Long-Range Correlations and Elliptic Flow	18
6.1. New directions	20
7. Conclusions and Outlook	21

1. Introduction

The LHC is, since it became operational, the energy frontier of particle physics. It is a diverse laboratory where:

- the standard model is being tested to impressive precision.
- the search for physics beyond the standard model is ongoing in numerous final states.
- the microscopic phenomenology of the quark-gluon plasma is being tested.

A common denominator of these activities is that they all depend on our understanding of the microscopic laboratory itself: the proton-proton (pp) collision. The protons are build up of quarks and gluons, and their partonic interactions are described by quantum chromodynamics (QCD). For inelastic collisions, one can have diffractive collisions, where no color charge is exchanged, or non-diffractive collisions, where color charge is exchanged. Here we will primarily focus on the non-diffractive collisions. In pp collisions, at the high energy of the LHC, several microscopic interactions will usually occur in each collision and each of these subcollisions can be characterized by the four-momentum transfer, Q^2 . When Q^2 is large we call the interaction hard and we can typically utilize perturbative QCD to describe it (1). However, when the Q^2 is low and the interaction is soft we reach the non-perturbative regime of QCD where we do not know how to calculate observables rigorously from first principles and we instead have to rely on phenomenological models and data-driven scaling relations to interpret the data. This review focuses on the same soft QCD in two regimes: 1) when all subcollisions are soft and the collision itself is therefore soft. This turns out to be the case for the bulk of pp collisions at LHC. 2) the soft subcollisions associated with one or more hard subcollisions, which is denoted the underlying event (UE).

Soft QCD is, like the LHC itself, a diverse research area. For some researchers at LHC, the soft QCD is an “annoying” background to their hard signal and the goal of tuning

phenomenological models is to describe this background as precise as possible. For others, the soft QCD is the signal and it has turned out that the LHC is a discovery laboratory, which we will try to highlight in the later sections of this review. When it comes to theory, soft QCD seems to find itself in a difficult situation: to be able to compare precisely with data one essentially has to use full pp generator models. However, most people working on understanding details of the soft pp collisions from first principles are often unwilling or do not have the resources to include their developments in these “simpler” models. This is hopefully something that will change in the coming years because as we hope to show, the field of soft QCD has never been more exciting than it is now and there will likely not be a better opportunity to study soft QCD in the next two or more decades.

Let us now try to explain what we mean with soft QCD in more detail. As perturbative QCD only describes quarks and gluons while hadrons are measured, there is always non-perturbative QCD involved in any QCD calculation, but this is not what we are particularly focused on here. Here we are rather interested in the physics dominated by the soft subcollisions. What scale Q^2 is then soft? One would naively expect that for $Q^2 \gg \Lambda_{QCD}^2$, where $\Lambda_{QCD} \approx 200$ MeV, the subcollision could be described by hard QCD, e.g., as a $2 \rightarrow 2$ partonic scattering. This would suggest that when we have particles with transverse momentum $p_T \gg \Lambda_{QCD}$ then they are the result of hard scatterings. However, this is not what we find experimentally. In fact, as we discuss in this review, there are many indications that the behavior of baryons, such as protons, remains distinctly different from hard QCD predictions out to $p_T \approx 8 - 10$ GeV/ c . This is a big surprise of LHC and one that is still not fully understood. So the soft scale is not set in stone but it seems that most particles with $p_T \leq 1 - 2$ GeV/ c are produced in soft processes, while one has to go to $p_T > 10$ GeV/ c to be in the fully hard regime, and so these are good experimental numbers to have in mind.

In this concise review paper, we aim to provide both an accessible introduction to soft QCD, supplemented with references for further reading, and a discussion of an eclectic selection of results and open questions that we find particularly intriguing. However, the expansive scope of soft QCD inevitably means that not all relevant topics could be addressed in detail. The structure of the paper is as follows: Section 2 offers a brief historical introduction to soft QCD physics. Section 3 presents an overview of contemporary models employed in physics analyses. Section 4 provides details on the methodology for studying multi-parton interactions and evaluates the performance of UE tunes in Monte Carlo event generators. Section 5 examines the production of identified particles in greater depth, while Section 6 focuses on the phenomenon of collectivity. Finally, Section 7 concludes with a discussion of future prospects in the field.

2. A Brief Historical Introduction

Soft QCD has been studied from early experiments at fixed-target facilities to modern high-energy colliders. The measurement of cross sections, as well as multiplicity distributions and longitudinal and transverse momentum (p_T) spectra gained most of the interest, see for example Ref. (2, 3) for a pre-LHC overview.

Before the advent of QCD, Regge theory (4) offered a framework to discuss hadronic cross sections. Central to this model is the Pomeron, which effectively captures the exchange of vacuum quantum numbers in soft QCD interactions. At high energy, the total hadronic cross section is dominated by Pomeron exchange and is predicted to rise with centre-of-mass energy as s^ϵ , where $\epsilon \approx 0.08$ is a small positive exponent. This growth of the cross section

can be related to the $x^{-\lambda}$ increase of parton densities in the proton towards small Bjorken- x values (5), with $x \propto \frac{1}{\sqrt{s}}$ and λ a function that depends on Q^2 .

This simple power-law rise would eventually conflict with the Froissart-Martin unitarity bound (6), which constrains the growth of cross sections to a $\ln^2 s$ dependence. Even though the cross sections measured at the LHC remain significantly below this limit (numerically still a factor ~ 100 below this bound (7)), the ratio of the elastic to total cross section (≈ 0.3 at LHC energies) increases with \sqrt{s} and is approaching the theoretical maximum of $\sigma_{\text{el}}/\sigma_{\text{tot}} = 0.5$ for a black disk. To account for the observed energy dependence, the exchange of multiple Pomerons must be considered. In terms of parton densities this could be connected to non-linear effects occurring below the saturation scale Q_s (8). This scale increases with center-of-mass energy and reaches $\sim 1-2$ GeV/ c for protons at the LHC, and higher for heavy ions. Experimental results from the LHC and other high-energy colliders confirm that total and elastic cross sections are in agreement with a log-square rise (see Figure 1).

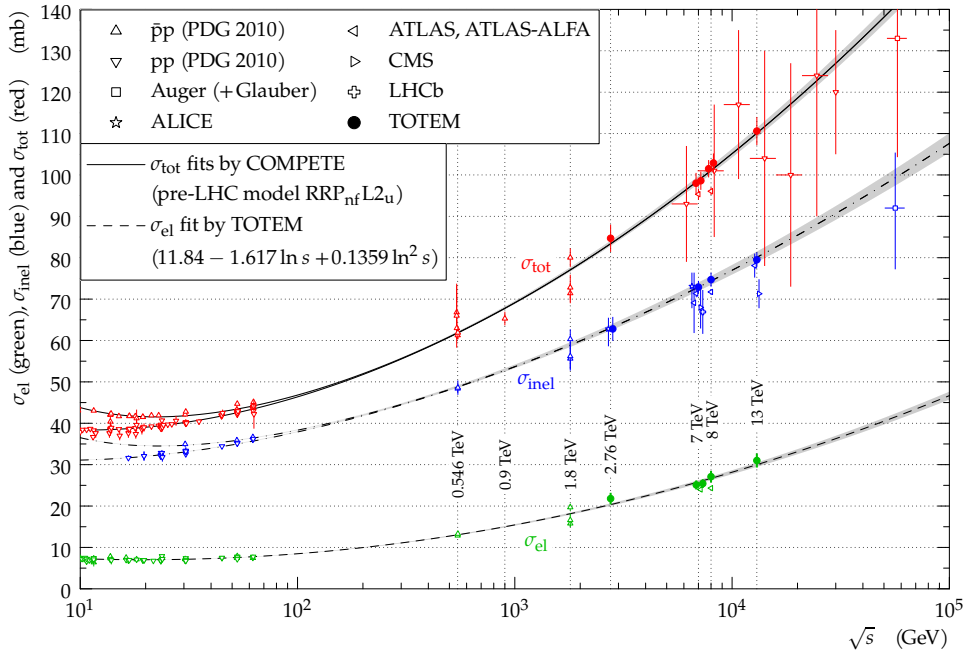


Figure 1

Overview of elastic, inelastic, and total cross sections for pp and p̄p collisions as a function of center-of-mass energy, \sqrt{s} (taken from (9)).

Particle production in inelastic collisions is linked to the elastic cross section via the optical theorem, which connects the imaginary part of the forward scattering amplitude to the total cross-section. In Regge theory, this connection introduces cut Pomeron-exchange diagrams, which result in multiple particle production chains (10). Energy-momentum conservation dictates that a hadronic system with invariant mass M will fragment into final-state particles with rapidities ranging between $\pm \ln(M/m)$ in the center-of-mass system, where m is the mass of the lightest final-state particles, typically pions. The full

rapidity distribution will thus be described by a superposition of rapidity distributions of individual production chains with different invariant masses, with maximal rapidity given by $\pm \ln(\sqrt{s}/m_p) \approx \pm 9.6$ for LHC energies of $\sqrt{s} = 13$ TeV. This framework is crucial for understanding multi-particle production in high-energy hadron collisions, as it illustrates the strong connection between the saturation of cross sections and parton densities on one side, and the emergence of multiple particle production systems on the other.

The multiplicity distribution gives the probability that a certain multiplicity is observed in a pp collision and is only measurable for charged particles. The observed particle multiplicity distribution follows approximately a negative binomial distribution, which captures the overdispersion seen in the data (i.e., the variance of the distribution is larger than the mean). In many cases, the multiplicity distributions exhibit long tails, indicating rare events with exceptionally high particle production.

In the early days of soft QCD studies, Koba-Nielsen-Olesen (KNO) scaling (11) was observed in particle multiplicity distributions. KNO scaling posits that the normalized multiplicity distributions should collapse into a single universal curve when scaled by the mean multiplicity, implying that particle production has a universal behavior across different energies. This phenomenon was initially supported by experimental data from lower-energy collisions. However, as measurements at higher energies were conducted, particularly at the LHC, a significant violation of KNO scaling was observed, as illustrated in **Figure 2**(left). The superposition of multiple distinct topologies with varying average multiplicities broadens the overall multiplicity distribution. Consequently, the breakdown of KNO scaling suggests that particle production cannot be explained by a single component or mechanism but instead points to a multi-component structure in the final state.

The p_T -spectra describe the average distribution of particles as a function of p_T . The spectra are typically normalized as an invariant yield, e.g., $1/(2\pi p_T) d^2 N/(dy dp_T)$, where y is the rapidity, and sometimes they are normalized to the cross section, σ , instead of per event. The p_T spectra typically display a power-law behavior at high p_T and an exponential drop at low p_T . This behavior reflects the different underlying physical processes: soft interactions dominate at low p_T , while harder QCD processes contribute the tail at higher transverse momenta. Indeed, the large p_T behaviour can be captured by the concept of x_T scaling (12). Here, $x_T = 2p_T/\sqrt{s}$ is a dimensionless variable that scales the transverse momentum p_T by the center-of-mass energy \sqrt{s} . In hard scattering processes, it is expected that the spectra measured at different collision energies should collapse onto a universal curve when plotted as a function of x_T . This scaling behavior reflects the self-similar nature of particle production processes. The violation of x_T scaling in the soft region indicates that purely perturbative approaches are insufficient to describe the entirety of the spectrum, and non-perturbative effects and multiple scattering processes must be included for a complete picture of particle production. Interestingly, the absolute p_T threshold below which non-perturbative effects are important appears to increase with centre-of-mass energy, reaching values above ~ 10 GeV/ c at the LHC, as can be seen in **Figure 2** (right).

In summary, even before QCD, Regge theory had introduced the idea of producing multiple particle chains. Modern Monte Carlo event generators therefore incorporate the concept of multiple parton interactions (MPI), where multiple partons within colliding protons can interact independently.

The LHC provides a unique opportunity to study soft QCD. At higher center-of-mass energies, the importance of MPIs increases, significantly contributing to the particle multiplicity. MPIs thus account for both the rapid increase in average multiplicity and the

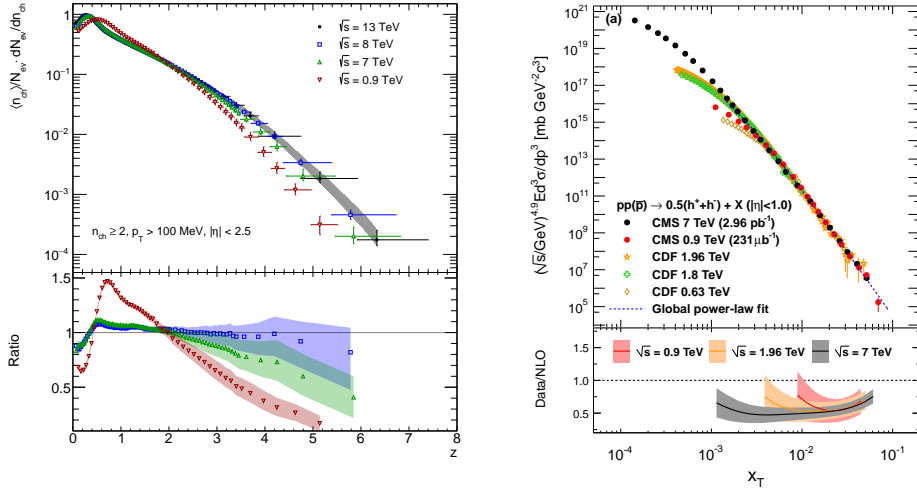


Figure 2

(left) KNO scaled primary charged-particle multiplicity distributions from the ATLAS experiment as a function of the scaled multiplicity for various centre-of-mass energies, together with their ratio to the $\sqrt{s} = 13$ TeV distribution (taken from (13)); (right) Inclusive charged particle invariant differential cross section from the CMS and CDF experiment as a function of the scaling parameter x_T for various centre-of-mass energies, together with their ratio to NLO calculations (taken from (14)).

greater variability in charged particle counts observed at the LHC and other high-energy colliders.

3. Phenomenological Modeling Perspectives

As we have seen in the last two sections, some features of soft QCD results can be understood in terms of QCD-inspired scaling relations and/or fits. However, to go towards quantitative descriptions of the measurements one needs phenomenological models that generate full events. The most popular phenomenological models used to describe pp collisions at LHC have been explained in detail in Ref. (15). Here, we will give a brief introduction to the main basic elements of soft QCD modeling only, to highlight the major differences between models and setup the discussion in the later sections.

Monte Carlo event generators incorporate detailed models to simulate soft pp collisions and the underlying event. At the partonic level, the most important ingredient in the models are MPIs as they primarily determine the activity and structure of the event (16). Here and in the following we always refer to the soft QCD part of the event. Possible hard scatterings will of course also affect the activity and structure but for the soft QCD observables we are interested in in this review, we typically can get around this issue, e.g., by looking in the transverse region, see Sec. 4.1. To accurately describe data one also has to include possible coherence effects between different interactions, e.g., color reconnection (CR) (16). The final important model ingredient that we will discuss is hadronization where

it is also important to handle the color connection to beam remnants.

The models we will mainly focus on here are PYTHIA (17), HERWIG (18), and EPOS (19, 20). The first two generators are the most popular pp generators at LHC, which includes a detailed handling of soft QCD, and they are systematically compared to LHC data at the MCPLOTS website <https://mcplots.cern.ch/> (21). The final generator, EPOS, is different from the other generators in that it also contains the partial formation of a quark-gluon plasma (QGP) in pp collisions.

3.1. Multiple-Parton Interactions

Let us first discuss this in a more abstract sense that can apply to all models. MPIs are in all cases treated as a sum of incoherent subcollisions, typically $2 \rightarrow 2$ partonic interactions. The QCD cross sections for these individual subcollisions diverge as $p_T \rightarrow 0$, ultimately exceeding the total cross section. This is not inherently problematic, as the ratio of the partonic QCD cross section to the total cross section can be interpreted as representing the number of MPIs occurring. Nonetheless, to prevent the cross sections from becoming unphysically large at low p_T , they must be regularized. This regularization can be linked to color screening, which limits the resolution of individual partons, as implemented, for instance, in PYTHIA, or to initial-state saturation effects, as done by EPOS.

Let us focus on a concrete example. In PYTHIA, subcollisions are modelled as $2 \rightarrow 2$ partonic processes and a transverse momentum cut-off scale, p_{T0} , is introduced to regularize the cross section:

$$\frac{d\hat{\sigma}}{dp_T^2} \propto \frac{\alpha_S^2(p_T^2)}{p_T^4} \rightarrow \frac{\alpha_S^2(p_{T0}^2 + p_T^2)}{(p_{T0}^2 + p_T^2)^2}, \quad 1.$$

where p_{T0} depends on the collision energy:

$$p_{T0}(s) = p_T^{\text{ref}} \left(\frac{\sqrt{s}}{\sqrt{s_0}} \right)^\epsilon, \quad 2.$$

with p_T^{ref} and ϵ as tuneable parameters. One finds that p_{T0} increases with energy, which is expected due to the increase of low- x partons in the proton wavefunction, and is of order 2 GeV/ c at LHC, i.e., we are only sensitive to length scales smaller than 0.1 fm, which is much smaller than the proton radius. Note that in a saturation picture, p_{T0} is related to Q_s . Additionally, an impact parameter dependence is introduced, making the number of MPI reliant on the spatial overlap of the protons' transverse profiles so that central collisions produce more MPIs than peripheral ones.

3.2. Intrinsic transverse momentum and initial and final state radiation

Intrinsic transverse momentum (k_T) represents the perpendicular momentum component of partons within nucleons and plays a critical role in modeling non-perturbative QCD effects. In processes like Drell-Yan production, intrinsic k_T influences the low p_T spectrum of dileptons, while initial state radiation (ISR), which describes gluon emissions by partons before hard scattering, introduces perturbative QCD corrections at higher p_T . Intrinsic k_T values on the order of 1 – 2 GeV/ c , increasing with center-of-mass energy, were determined through an analysis of Drell-Yan data (22).

Final state radiation (FSR), involving gluon emissions from outgoing partons post-scattering, further redistributes momenta. Together, intrinsic k_T , ISR, and FSR provide a

comprehensive framework for simulating angular and momentum correlations in the final state. A notable example is jet production in high-energy collisions, where these effects contribute to deviations in azimuthal correlations, particularly in back-to-back jet configurations (23).

Monte Carlo event generators model ISR and FSR as a parton shower, where successive emissions are computed based on the Altarelli-Parisi splitting functions that describe the probability of a parton splitting into a pair of partons. In ISR, each emission reduces the parton’s energy and modifies its transverse momentum, leading to a cascade of radiation that results in a more complex initial state. FSR accounts for the fragmentation of outgoing partons into hadrons, forming jets and shaping the final event topology.

PYTHIA employs an interleaved approach to handle MPI alongside ISR and FSR. In this method, MPI, ISR, and FSR steps are dynamically combined in a common ordering sequence. This approach enables PYTHIA to account for correlations and competition between these interactions, leading to a more accurate depiction of the particle production process.

3.3. Hadronization and color reconnection

Once the MPI model has generated a colored final state, it has to be hadronized. This is an area with substantial differences between generators. For example, PYTHIA uses the Lund string model and HERWIG uses a cluster model. An important assumption of most hadronization models is “Jet Universality”, which means that the final objects that hadronize, e.g., strings or clusters, and the parameters used in the hadronization of these objects are universal. This implies that the parameters can be tuned using better understood data from $e^+e^- \rightarrow q\bar{q}$ so that their parameters are fixed for pp collisions. Finally, each generator also have to implement a scheme for how it handles the beam remnants in the hadronization process.

To accurately describe data it turns out that one has to add a step in between MPIs and hadronization where one breaks the incoherence of the MPIs. This is very important for describing the observed rise of $\langle p_T \rangle$ with multiplicity in pp collisions, as will be explained next. The multiplicity grows with the number of MPIs. If MPIs were incoherent, then they should on the average produce the same $\langle p_T \rangle$ because of Jet Universality and so there would be no rise of $\langle p_T \rangle$ with multiplicity. PYTHIA, for example, has a color reconnection (CR) model that adjusts the color flow between partons originating from different scatterings to minimize the total string length. This allows PYTHIA to describe the $\langle p_T \rangle$ increase. This breaking of incoherence is critical for describing the data and it turns out that even more advanced models are needed to describe the strangeness enhancement discussed in Sec. 5.2. Surprisingly, CR is also relevant to W^+W^- pair production in e^+e^- annihilation when the W bosons decay hadronically, and influences the systematic uncertainties in the measurement of the W mass. We will return to the more advanced CR schemes later in the text when we discuss the data that requires the models to introduce them.

The most extreme way to break the incoherence is found for EPOS. EPOS assumes that a QGP will form in the dense regions of a pp collision (those regions with many MPIs). The MPI subcollisions are therefore classified into two distinct groups: a non-QGP “corona”, which hadronize more or less independently, while subcollisions in a dense QGP region forms a common “core” that expands hydrodynamically and cools before hadronizing according to

the statistical thermal model ¹. In EPOS, the rise of $\langle p_T \rangle$ with multiplicity occurs because the importance of the core grows with multiplicity and because the expansion of the core will give rise to a radial flow that boosts the p_T . For example, assuming a hadron is produced with zero p_T in the QGP rest frame, it will end up with the following p_T in the laboratory frame:

$$p_T = \gamma \beta_r m, \tag{3}$$

where β_r is the radial flow velocity and m is the mass of the particle. As can be seen, this will introduce a mass dependence for the $\langle p_T \rangle$ growth with multiplicity, which is also observed in data, see for example (25). Importantly, it can be shown that the CR of PYTHIA effectively also produce a boost like Eq. 3 and therefore also produce this mass dependence (26). This opens a big question of to what degree CR and hydrodynamics is at work in pp collisions. Is it for example all CR and there is no QGP or is it all hydrodynamics and there is no CR? This question is still not resolved and is probably the biggest open questions when it comes to soft QCD at the LHC.

3.4. Summary of Generators

Table 1 Summary of the main differences between the pp generators covered in this review. The structure of the table follows the structure of the previous subsections.

Generator	Ref.	Soft MPIs	CR or similar	Hadronization
PYTHIA 8	(17)	2 → 2 partonic	CR, Ropes, Junctions	Lund strings
HERWIG 7	(18)	2 → 2 partonic	Statistical CR, baryonic R	Clusters
EPOS LHC	(19)	Pomeron exchanges	Core-corona model	Thermal core

Table 1 summarizes the features of the generators that were discussed previously in this section. For EPOS, the relatively old EPOS LHC version is listed while there is also a more modern EPOS 4 version (20). However, currently EPOS LHC is the most used version at LHC.

The main differences between the generators are for the CR and hadronization, which are often interleaved: the CR implemented in PYTHIA is handled at the string level while the core-corona formation in EPOS controls the hadronization. Even CR concretely leads to modified hadronization in the models, the physics interpretation is not clear and one can also think of CR as a modification of the MPIs, e.g., to mimic saturation.

For modeling of MPIs there are alternative theoretical frameworks such as the Color Glass Condensate (CGC), which is derived from first principles, see (27) for an overview. The CGC takes advantage of the growth of low- x gluons in the proton wavefunction with the center-of-mass energy. Because of these dense gluon fields at LHC, the MPIs are in the CGC framework modeled as collisions between classical fields and the regularization enters via the saturation scale, Q_s . As the LHC is the energy frontier for the foreseeable future, it would be interesting to understand better if such a framework can be incorporated into pp generators and what the observables that would be most affected at the LHC would be and/or if there would be unique predictions of such a framework.

¹The statistical thermal model has been hugely successful in describing integrated particle yields in AA collisions, see for example Ref. (24).

4. Multiparton Interactions and Underlying Event Tunes

Inspired by Regge-Gribov theory, which allows for events with multiple cut Pomerons—each producing a sequence of low- p_T hadrons—and motivated by experimental observations, Monte Carlo event generators incorporate detailed models to simulate the underlying event. These models account for contributions from MPI, intrinsic k_T , ISR and FSR, color reconnection, and beam-beam remnants (BBR). The models introduce several free parameters, which are tuned to minimum bias and UE data by experimental collaborations. Specific observables have been designed to be sensitive to UE activity. Current tunes successfully describe the underlying event across various final states, including multijet, Drell-Yan, Z and W boson production, and top quark pair production. An excellent review of MPI at the LHC can be found in (28).

4.1. Underlying Event Observables

A widely used approach (29) for systematically measuring the underlying event in pp collisions relies on identifying a leading object in the event, which could be the charged particle or jet with the highest transverse momentum. This leading object is associated with the hard scattering of the event. The transverse momentum of the leading object, p_T^{leading} , is used as a reference for UE measurements.

The event is divided into different regions of azimuthal angle ϕ relative to the leading object's direction:

- The *toward* region is defined as the direction of the leading object ($|\Delta\phi| \leq 60^\circ$), where contributions mainly come from the hard scatter.
- The *away* region is located in the direction opposite to the leading object ($|\Delta\phi| > 120^\circ$), and typically contains the recoil from the hard scatter.
- The *transverse* regions are defined as the regions perpendicular to the leading object ($60^\circ < |\Delta\phi| \leq 120^\circ$), this is where the UE activity is expected to dominate. Since it is far from both the hard scatter and its recoil, it primarily contains contributions from MPI, ISR, FSR, and BBR.
- To further refine the measurement, the transverse region can be split into two subregions: *transMIN* is the transverse region with the minimum activity and is particularly sensitive to MPI and BBR since it minimizes the contribution from ISR or FSR, and *transMAX* which is the transverse region with the maximum activity which may include ISR and FSR in addition to MPI and BBR. By comparing *transMIN* and *transMAX*, the method can distinguish between ISR/FSR and MPI contributions – e.g. by computing the difference of *transMAX* and *transMIN*, one can single out the contribution from ISR/FSR.

Two main observables are studied to characterize the underlying event in these regions: multiplicity N_{ch} and the scalar sum of transverse momentum $\sum p_T$ of the charged particles. Although multiplicity is not an infrared-safe observable, it is closely linked to the number of MPIs. In contrast, the sum of transverse momentum is primarily governed by the overall energy flow distribution w.r.t. the leading object. These quantities are then measured as a function of p_T^{leading} .

4.2. Monte Carlo Tunes

UE tunes are derived using tools such as PROFESSOR (30) and RIVET (31). These tools enable experimental collaborations to compare simulated event samples generated by Monte Carlo event generators, like PYTHIA and HERWIG, with real data. PROFESSOR is used for automated tuning: it parametrizes the MC generator’s predictions and fits them to minimize the difference between the simulation and experimental data. RIVET (and MCPLOTS) provides a framework for comparing distributions of observables sensitive to the underlying event, such as charged-particle multiplicities and transverse momentum sums, between data and simulation. This combination allows experiments to derive the best-fit parameters for MC generators, resulting in “tunes” that accurately describe the underlying event across a range of processes and energies. Through this process, different tunes, that significantly improve the reliability of simulated collisions at the LHC, have been obtained by various authors. In the next section we compare observables to the following specific tunes obtained by ATLAS and CMS:

- A significant contribution is the CP5 tune (32) for PYTHIA 8, which was created by CMS using the parton distribution functions (PDFs) from NNPDF 3.1. The CP5 tune is a multipurpose tune, aiming for a consistent description of underlying and minimum bias observables at several collision energies and a reliable prediction of the UE simulation in various processes when merged with higher-order ME calculations. The tune was extensively validated and showed that using NNLO PDFs significantly improves the modeling of both soft and hard processes in proton-proton collisions, making CP5 one of the most reliable tunes for high-precision LHC measurements.
- One of ATLAS’ widely used tunes is the A14 tune (33) for PYTHIA 8, which was developed based on a combination of observables from both minimum-bias events and Drell-Yan processes. The A14 tune uses the NNPDF 2.3 LO PDF set. It was optimized using data from minimum-bias and UE observables collected at a center-of-mass energy of 7 TeV. The tune was validated against a wide variety of processes, including Z-boson production and jet production, demonstrating good agreement with experimental data.

4.3. Tune validation

Figure 3 demonstrates how different tunes reproduce various UE observables. The top row presents the average charged-particle multiplicity and p_T sum in the transMIN region as a function of the leading charged particle’s p_T . This region is predominantly sensitive to MPI. Both the ATLAS and CMS tunes provide a reasonable description of the ATLAS data, although slight discrepancies appear around the turn-on region at $p_T^{\text{lead}} \sim 7 \text{ GeV}/c$. The bottom row shows these same distributions in the transDIFF region, which emphasizes initial-state and final-state radiation (ISR/FSR). While the tunes generally succeed in capturing the p_T sum, they tend to overestimate the charged-particle multiplicity. This outcome highlights the ongoing complexity of UE tuning and shows that certain tensions remain in accurately modeling these observables.

CMS has conducted detailed studies of color reconnection effects within the underlying event (34) and explored different models of color reconnection implemented in PYTHIA 8, particularly those based on MPI, QCD-inspired models, and gluon-move models. These studies compared the default CP5 tune (which uses the MPI-based CR model) with alternative CR models, and showed significant potential for improving the description of soft

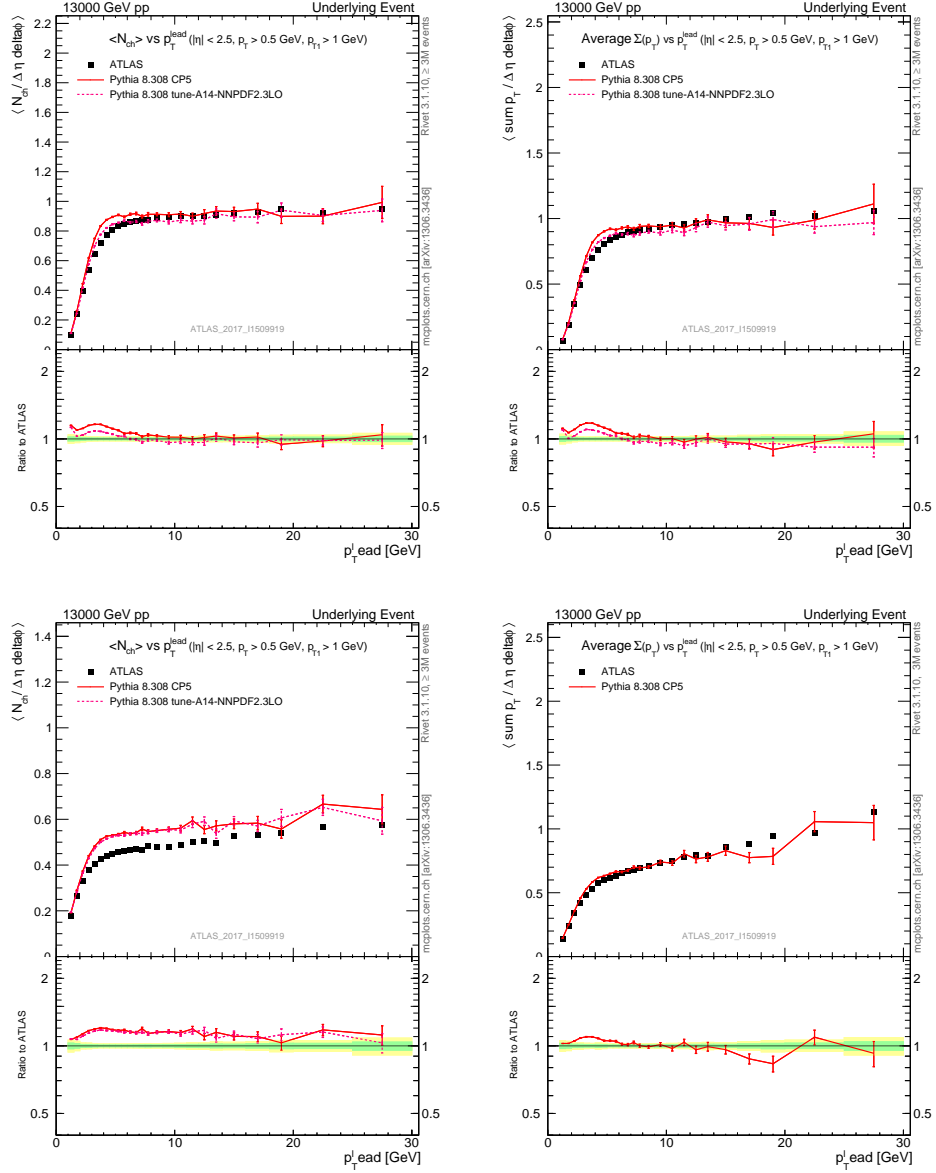


Figure 3

UE observables are shown as functions of the transverse momentum of the leading charged particle. The top row presents the average charged-particle multiplicity (left) and transverse momentum sum (right) in the transMIN region. The bottom row displays the same observables for the transDIFF region. These plots were obtained using the `mcplots.cern.ch` tool.

particle production and UE observables, providing a better fit to charged-particle multiplicity data and event shapes in the transverse region.

ATLAS has conducted UE studies focusing on strange hadron production (35), including K_S^0 , Λ , and $\bar{\Lambda}$, which are sensitive to hadronization effects. These studies revealed that

while the current MC models generally describe the data well, discrepancies remain in certain kinematic regions. For example, the observed yields of strange hadrons and their correlations with charged-particle multiplicity in the transverse region, used as a proxy for the number of MPIs, showed tensions with the predictions from the standard tunes.

It is important to note that, beyond the specific UE observables discussed in Section 4.1, other properties of the final state are also affected by soft QCD. For example, measurements of transverse sphericity, as reported in (36, 37), show that sphericity increases with charged multiplicity, which correlates with the number of MPI. This effect is consistent with the expectation that additional MPI contribute to a less jet-like event topology. However, current tunes tend to underestimate this impact, predicting more jet-like final states than observed. This is confirmed in (38) where the average p_T of particles in jet-like events is overestimated by models, while the same observable is well described in events by more spherical final state topologies.

Rather than focusing solely on particle activity in the transverse plane, one can examine separations in rapidity. First measurements of the underlying event at forward rapidity at $\sqrt{s} = 0.9, 2.36,$ and 7 TeV were reported in (39). These studies were extended to $\sqrt{s} = 13$ TeV, for instance in (40, 41), providing valuable data for further validation of underlying event (UE) models.

Similar arise findings from studies of forward-backward (42) and long-range correlations in rapidity (43), which decrease with increasing charged multiplicity. Notably, these long-range correlations appear to be universal across different collision systems, including proton-proton, proton-lead, and lead-lead interactions.

Finally, it is worth noting that the tuning efforts discussed in this section are based on the assumption that MPIs are azimuthally isotropic, as this is how they are implemented in Monte Carlo simulations. However, there is no inherent reason to rule out the possibility of MPIs being correlated with a preferred azimuthal direction, such as the collision plane. As demonstrated in (44), introducing such azimuthal correlations can reproduce the long-range, near-side correlations in proton-proton collisions initially observed by CMS (45) (see Sec. 6).

5. Particle Production of identified particles

In this section we will focus on measurements of identified hadrons. As the review is focused on soft particle production, we will limit ourselves to hadrons containing up, down, and strange quarks and their associated antiquarks. There are three additional complementary aspects of particle production that can be studied with identified hadrons:

- Effects related to mass.
- Effects related to quark content, e.g., strangeness.
- Baryon vs. meson differences.

While the mass typically enters each model in a straightforward way, the latter two provide fundamental insights into how quark masses and hadron type affects particle production. For this reason they will be the focus here. However, it should be pointed out that even mass and baryon vs. meson differences are well separated in models they are not so easy to separate experimentally as baryons typically are heavier than mesons. This means that some experimental observations can be explained in one model by a mass effect and in another model by a baryon vs. meson effect.

Let us start by focusing on the biggest paradigm change that has resulted from measurements of identified particle production at LHC. As we discussed in Sec. 3.3, the traditional pp paradigm with MPIs and Jet Universality leads to pp collisions where the properties of subcollisions are independent of multiplicity and constrained using data from $e^+e^- \rightarrow q\bar{q}$. For this reason, one expects that particle ratios of strange hadrons to charged pions should not depend substantially on particle multiplicity. It was therefore a big surprise when ALICE measured that the p_T -integrated ratios of cascades to charged pions, $\Xi(ssd)/\pi$ and $\Omega(sss)/\pi$, are significantly enhanced with multiplicity even in pp collisions (46). The ALICE results on strangeness enhancement have *irreversibly* falsified the traditional pp paradigm. For models to describe the data, one therefore has to allow for significant final-state interactions that break the picture of a pp collision as an almost incoherent sum of subcollisions. We stress this here (and return to it later) to emphasize that we now are in a time period where models are struggling to explain the data and where one can expect fundamental breakthroughs in our understanding in the coming years.

The rest of this section is organized as follows. First we will examine how well pQCD describes p_T -spectra of identified particles at LHC energies. After this we review experimental measurements of different particle species and their production rates. Finally we will discuss baryon production.

5.1. Lessons from hard production

One typically expects that perturbative QCD can describe particle production at intermediate to high p_T , e.g., $p_T > 3 - 4 \text{ GeV}/c$. Perturbative QCD (pQCD) requires two inputs: parton distribution functions (PDFs) and fragmentation functions (FFs). The PDFs are known to reproduce several observables, e.g., jet production and backgrounds in searches for new physics, so when comparing pQCD calculations with identified spectra one is mostly testing the identified FFs. A big surprise from the LHC has been that it has been very difficult for pQCD to describe spectra of neutral pions and charged pions, kaons and protons, see for example Refs. (47, 48). As suggested in Ref. (49), one of the problems could be that in some cases there are sizable non-perturbative effects for $p_T < 10 \text{ GeV}/c$, something we return to in the next section. Recently it has been possible to obtain a new set of FFs that provide a good description of both charged and neutral pion spectra at LHC (50). Note that in a string picture one can find large non-perturbative corrections to hadron production, even the partonic production is perturbative and so there is a fundamental tension with the idea of universal FFs (51).

5.2. Review of identified particle spectra and production rates

Where the studies of identified particles shine are when the evolution of different particle spectra are compared. For this reason, we will focus here on particle ratios as a function of final-state charged-particle multiplicity, $\langle dN_{\text{ch}}/d\eta \rangle$.

ALICE is the experiment at the LHC with the best capabilities for studying identified particle production due to its PID capabilities, low magnetic field, and low material budget. ALICE has recently published a long review of the results from LHC, which also includes soft QCD in pp collisions (52). Here, we focus on a few selected results from this as well as newer results.

For particle ratios as a function of p_T , ALICE has found that at low and intermediate p_T there can be a substantial evolution with $\langle dN_{\text{ch}}/d\eta \rangle$ in pp collisions. This is particularly

true for ratios of baryons to mesons, e.g., p/π and Λ/K_s^0 , while some ratios, such as K/π , are almost independent of p_T , see for example Ref. (53). The baryon-to-meson ratios have a multiplicity dependence for $p_T < 10 \text{ GeV}/c$. Some of this multiplicity dependence at low and intermediate p_T is expected from both CR and radial flow, c.f. Eq. 3, and this is likely why it has been difficult to explain identified spectra with pQCD and also why one can find a good set of FFs for pions, due to their low mass. However, it is not clear that radial flow or color reconnection can explain all the changes in particle ratios with multiplicity at intermediate p_T and therefore it could be that one has to include quark recombination effects (54). In recombination models, baryons (mesons) “combine” from three (two) co-flowing quarks and so baryons naturally end up with significantly higher p_T than mesons. This could also explain why it is mostly baryon-to-meson ratios that are modified. For completeness, we note that this mechanism could also play a central role in understanding the production of heavy flavor baryons, see for example Refs. (55, 56). It will therefore be interesting to see if one can validate or falsify this idea in the coming years.

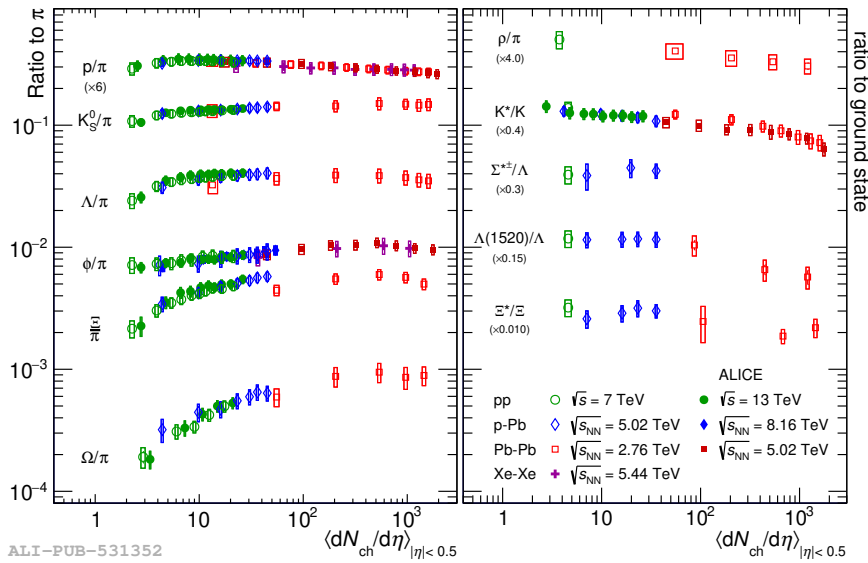


Figure 4

The p_T -integrated yield ratios to pions ($\pi^+ + \pi^-$), left, and p_T -integrated yield ratios between resonance and corresponding ground state, right, are shown as a function of $\langle dN_{ch}/d\eta \rangle$ measured in $|\eta| < 0.5$ demonstrating universality across collision systems and beam energies. Figure taken from (52).

The ALICE results that have had the biggest impact on soft QCD are the ratios of integrated particle spectra where it has been found that they only depend on $\langle dN_{ch}/d\eta \rangle$, irrespective of collision system (pp, pA, and AA) and beam energy, as shown in Fig. 4. For the cases studied, it has even been found that p_T -differential ratios have this universal scaling for a given p_T (53).

It is important to stress here that one has to be careful with how one defines multiplicity because it is easy to introduce “selection” and “jet” biases, which are both caused by *local* fluctuations in the *charged* particle density. These biases can affect both the measurements

of the identified particles and the $\langle dN_{\text{ch}}/d\eta \rangle$. For these studies, the multiplicity selection is done using forward detectors while the identified particles and the $\langle dN_{\text{ch}}/d\eta \rangle$ are measured at mid-rapidity to avoid these biases. Understanding and controlling these and similar biases is a big challenge in ongoing and future experimental investigations using new observables.

Returning to Fig. 4, one notices that the main changes in particle ratios with $\langle dN_{\text{ch}}/d\eta \rangle$ are for the strange hadrons including the ϕ meson, and in particular for the multi-strange baryons. This is commonly referred to as strangeness enhancement. Several measurements have been carried out to pinpoint the origin of the strangeness enhancement. By measuring particle ratios inside and outside of jets it has been established that the strangeness enhancement is mostly produced in the underlying event (57). It is challenging to constrain precisely the strangeness enhancement for hard jets as it is expected to be mainly located at low p_{T} where the underlying event dominates. There are indications that at least for “jets” with intermediate- p_{T} leading particles one can observe an enhancement (58). A modified version of transverse sphericity, designed to minimize the biases discussed above, has been used to study particle production in high multiplicity events (59). In this study it was found that one can reduce the strangeness enhancement for fixed $\langle dN_{\text{ch}}/d\eta \rangle$ by selecting “jet-like” events. On the contrary, it is not really possible to enhance the strangeness production significantly, which suggests that the bulk of high-multiplicity events are dominated by soft physics. This can also help explain the universal scaling observed in Fig. 4 because it suggests that the measurements in all cases are dominated by soft physics and it is only if one selects hard processes or events dominated by hard processes that one can break this scaling.

Let us now focus on the models. The pp models that can describe the strangeness enhancement have all had to implement some form of final state interactions.

In PYTHIA, more complicated forms of color reconnection has been implemented. Where ordinary color reconnection is important for describing the rise of $\langle p_{\text{T}} \rangle$ with multiplicity and the radial-flow-like effects in the data, this new color reconnection is centered around the formation of junctions (60), which are more likely to produce baryons, and ropes (61), which are more likely to produce strange hadrons due to an increased string tension. The current biggest challenge for PYTHIA is that, to explain the strangeness enhancement, one ends up with a general baryon enhancement due to the junctions that is not observed for protons, c.f. Fig. 4 and Ref. (62).

HERWIG has successfully described the strangeness enhancement by improving the way gluons fragment to $s\bar{s}$ and allowing three $q\bar{q}$ clusters close in phase space to reconnect to form a baryon-antibaryon pair (63). While these new mechanisms allow HERWIG to reproduce the strangeness enhancement, they predict enhanced strangeness production in transverse-sphericity-selected jet-like events, contrary to what is observed in the data (59). The reason for the enhancement in HERWIG appears to be the many mesons having parallel momentum vectors in jet-like events, resulting in enhanced “baryon reconnection”. As the “baryon reconnection” is reminiscent of quark recombination discussed above, this suggests that transverse sphericity analyses can be used to test these ideas if they can be implemented in generators.

When one introduces QGP formation, the change in particle ratios can be explained in two ways:

EPOS has a dense QGP-core and a dilute pp-model-like corona and the change with multiplicity is mainly driven by the growing importance of the core (19). Recently, a detailed analysis of the particle ratios has been done in EPOS 4 (64). There one also tested the effect

of hadronic scattering, which is found to have very little effect in pp collisions. The paper interestingly points out that while there is a continuity of particle ratios between pp and AA collisions, the $\langle p_T \rangle$ in AA collisions is significantly lower than in pp collisions. This is expected in EPOS because the core is smaller in pp collisions for the same $\langle dN_{\text{ch}}/d\eta \rangle$ and therefore expands more leading to larger radial flow.

Alternatively, assuming full QGP formation in all pp collisions, one can describe the change with multiplicity as the transition from a canonical to a grand-canonical thermal-model description, which can be done in many ways and with and without full strangeness equilibration, see for example Refs. (65, 66, 67). In these models, strangeness is not enhanced in large systems (AA) but canonically suppressed in small systems (pp). There are three challenges to these full QGP models in small systems and the proposed idea of strangeness suppression. 1) If strangeness is not equilibrated in a small system can we then really talk about a suppression? 2) In the basic version of the statistical thermal model, the ϕ is expected to be enhanced in small systems relative to other particles because it has $B = 0$, $S = 0$, and $Q = 0$ and therefore is never canonically suppressed. However, as can be seen in Fig. 4 the ratio ϕ/π increases with $\langle dN_{\text{ch}}/d\eta \rangle$ in pp collisions and so one likely has to treat the ϕ as doubly strange to explain this (66). 3) A potentially bigger problem is that none of these models are implemented as full event generators and so one can really only evaluate integrated ratios and not handle correlations or biases, which are important in pp collisions. It would be great if more resources in the field would go into formulating a full generator built around this idea. Without event generators, it is almost impossible to see how one can validate or falsify the interesting and perspective-changing idea of strangeness suppression in small systems.

5.3. Baryon production

Recently a new type of measurement has become available at the LHC where one directly studies the microscopic balance of quantum numbers, B , S , and Q , for Ξ baryons by other hadrons (68). The measured microscopic balance has turned out to challenge all models as it does not depend significantly on multiplicity indicating that the microscopic production of Ξ is more or less the same *independent* of the yield enhancement. For example, in PYTHIA the strangeness enhancement is mainly explained by junction formation, which can be observed in the balance results as one is much more likely to balance the baryon number of a Ξ^- by a \bar{p} than for the default diquark model, which requires one \bar{s} in the balancing antibaryon. However, junction formation naturally has a multiplicity dependence as it depends on the string density so that one expects changes in the Ξ balancing with multiplicity, which is not observed in the data.

As this type of measurement allows one to constrain the microscopic production mechanisms there is hope that similar measurements of other particle species can lead to new breakthroughs in our understanding of baryon production and hadronization in general.

An effect that is observed in data, but does not appear to be in any of the models, is that $B - B$ (and $\bar{B} - \bar{B}$) correlations are suppressed close in phase space (69). As the strangeness enhancement is mainly observed for strange baryons one could worry that we are overlooking essential pieces of information that could improve our understanding of baryon production. It would therefore also be interesting if CMS or ATLAS, which can measure Λ - Λ correlations over a much broader rapidity range than ALICE, would also study these

correlations.

6. Collectivity: Long-Range Correlations and Elliptic Flow

In large collision systems, the observation of anisotropic collective flow has been one of the most transformative measurements in the field of heavy-ion physics, see Ref. (70) for an overview. The observation of collectivity in pA and pp collisions, see for example Refs. (71, 72) for overviews, both raises questions about the origin of the flow and offers new possibilities in these fields. As the reference system in this case is AA collisions, we will first start by describing the physics there, see Ref. (70) for details.

The idea of flow is easiest to understand in the hydrodynamic paradigm. In hydrodynamics, the expansion of the QGP formed in AA collisions is driven by pressure gradients. As semi-central collisions have an anisotropic “elliptic” spatial distribution, the hydrodynamic expansion will lead to a momentum anisotropy that has its major (minor) axis along the minor (major) spatial axis. In general one can describe the final state by a Fourier series:

$$\frac{dN}{d\varphi} \approx \frac{N}{2\pi} \left(1 + 2 \sum_{n=1}^{\infty} v_n \cos(n(\varphi - \Psi_n)) \right) \quad 4.$$

where φ is the azimuthal angle, Ψ_n is the n -th order symmetry plane and v_n are the flow coefficients. The elliptic flow, v_2 , dominates AA collisions and is mainly driven by the average geometrical overlap and Ψ_2 is approximately the azimuthal angle of the impact-parameter vector. The triangular flow, v_3 , has turned out to be driven by event-by-event fluctuations, which means that Ψ_3 is independent of Ψ_2 .

Flow measurements have transformed the field of heavy-ion collisions in the following ways:

- The large magnitude of the elliptic flow requires a perfect liquid with a shear-viscosity-to-entropy density close to the universal value for a large class of strongly interacting quantum field theories (73). This has falsified the idea of a weakly coupled QGP and established the strongly interacting QGP, sQGP.
- The observation of large triangular flow indicates that event-by-event fluctuations in the initial state are important and can be probed with anisotropic flow and event-by-event flow fluctuations. This has even provided some sensitivity to the magnitude of subnucleonic fluctuations (74) that could be relevant for our understanding of pp collisions.

The important thing to understand is that a perfect liquid has as little entropy generation as possible, i.e., almost no diffusion or dissipation, and so it preserves information from the stages of the collisions that we cannot otherwise easily probe. This has allowed Bayesian analyses to constrain the equation of state and many other properties of the QGP (75).

In small systems, flow is difficult to observe, which can be understood in the following way. The correlations imprinted by flow are weak but present between all particles (global), while non-flow correlations, such as those resulting from (mini)jets and resonance decays, are strong but only involves few particles (local). For this reason, flow-induced correlations dominate for high multiplicities (AA collisions) while non-flow correlations dominate for low multiplicities (pp collisions), which also makes it impossible to measure the symmetry planes Ψ_n in pp collisions. In a recent review (72), the many different ways to extract flow

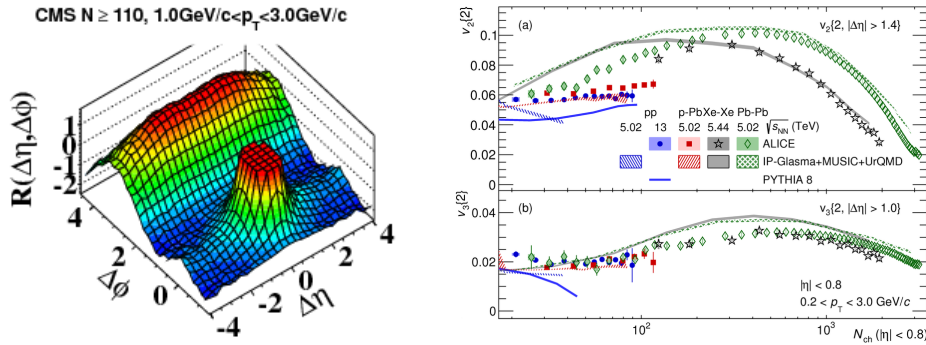


Figure 5

Left: the first observation by CMS of the near-side ridge in high-multiplicity pp collisions. Figure adapted from (45). Right: measurements of v_2 and v_3 by ALICE for pp, pA, and AA collisions using measured using two-particle cumulants with a pseudorapidity separation $|\Delta\eta| > 1.4$ and 1.0, respectively, chosen to suppress nonflow contributions. Figure adapted from (76).

in small systems have been described in detail. Here we shall just go through some of the main observations of flow in small systems at the LHC.

The first observation was the near-side ridge in very high-multiplicity pp collisions observed by CMS in 2010 (45), as shown in **Figure 5 left**. This was followed by the observation of the double ridge in p-Pb collisions by ALICE (77) and ATLAS (78). Since these first results, a lot of work has gone into refining the techniques to measure flow and ALICE has recently conducted a systematic study of flow across all systems (76). The study found that the flow coefficients v_2 and v_3 are similar for different systems, pp, pA, and AA, when compared at the same $\langle dN_{ch}/d\eta \rangle$ in the low-multiplicity region, see **Figure 5**. In this region, one expects the initial state geometry to be driven by fluctuations and therefore to be similar for all systems. The observation that the flow coefficients are the same therefore suggests that the origin of the flow is the same. It is worth to point out that the results with v_2 were validated in the same paper using using flow cumulants with two and three subevents (79), which is one of the most precise measurements of flow.

Now let us turn to discuss the origin of flow in small systems. For some time it appeared that the flow in small systems might be produced by initial-state effects, as predicted by the Color Glass Condensate (CGC) (80), but this has since then been disfavored both experimentally and theoretically. Experimentally, RHIC carried out a spectacular program of p-Au, d-Au, and ^3He -Au collisions with which they could demonstrate that initial-state effects could not explain the flow (81). Theoretically, it was recently realized that when one combines CGC calculations with final-state effects, needed to produce a hydrodynamic medium in larger systems, the long-range initial-state flow correlations disappear (82). This means that the only hypothesis that is currently valid is that flow in small system is to a large degree due to final-state interactions. As this is also what we expect to be the case for the strangeness enhancement discussed in the previous section, the two observations are consistent.

The main open questions when it comes to flow are the following ones:

- What are the smallest systems that can flow?
- How can we theoretically understand how flow arises in very small systems?

The surprising observation in pp collisions has been that there does not appear to be an onset of flow with multiplicity (72, 76). In fact, flow-like signatures have been observed even for multiplicities that are smaller than those of MB pp collisions (83). This has shifted the question of the possible onset of flow to different collision systems. Using LEP data at the Z peak, it has been found that flow does not appear to be present in $e^+e^- \rightarrow q\bar{q}$ collisions (84). However, results for higher LEP beam energies, above the $e^+e^- \rightarrow W^+W^-$ threshold, suggest that flow-like correlations are present there (85). Other types of systems that have been studied are ultra-peripheral collisions (UPCs) at LHC and ep collisions at DESY. In these systems, one expects that the γ^* will interact hadronically for low Q^2 and so they are relevant to compare with. ATLAS has observed flow in UPC γ^* -Pb events (86) and CMS has reported non-zero v_2 in γ^*p events (87), but finds that the magnitude is consistent with model predictions that have no collective effects. ZEUS and H1 have reanalyzed old data both for low and high Q^2 but neither ZEUS (88, 89) nor H1 (90) observes any signatures of collective flow. To use these systems to establish the onset of flow it would be good to see investigations of both UPC systems by a single collaboration and even discussions between analyzers at LHC and HERA to ensure that the different results are not caused by differences in analysis choices.

One of the biggest questions for small system has been the following: how can we form an equilibrated medium in these small systems? This is a very active and difficult theoretical topic with many breakthroughs. The first major breakthrough, resulting from efforts on several fronts, was the realization that hydrodynamics does not require thermalization but only hydrodynamization, see Ref. (91) for a recent review. In weakly-coupled kinetic theory one can study out-of-equilibrium systems in detail and build up a better understanding of hydrodynamization. There, one finds that systems first reach kinetic equilibration, then chemical and finally thermal equilibrium, see for example Ref. (92), and that the system can already be described by hydrodynamics when it is in kinetic equilibrium. When one estimates the system size (multiplicity) at which one can have hydrodynamic flow, it is found to be significantly bigger than the range of multiplicities where flow-like effects are observed in pp collisions (92, 93). It turns out that one can generate flow-like signals that are not hydrodynamic at lower multiplicities. An example of this is the escape mechanism where the flow-like signal is induced by an azimuthally asymmetric escape probability and only requires one interaction on the average (94). In fact, one can generate flow-like signals in this way even in realistic QCD kinetic theory (95). This is a fantastic result, but unfortunately it is sometimes interpreted as an indication that everything flows and that perfect-liquid-like behavior in pp collisions is not very special. Instead, the community needs to develop generators that can be compared apples-to-apples with data to see if this proposed mechanism is indeed a viable explanation. We think this is urgently needed as there are reasons to be skeptic: no onset of flow is observed in pp collisions while any weak-coupling calculation naturally has a finite mean free path. This makes it likely that strong-coupling physics is needed to explain the observed flow in pp collisions, which is difficult to calculate, but could make the flow in pp collisions perfect (vanishing mean free path). We therefore encourage heroic efforts to continue progress on this side as well.

6.1. New directions

CMS has recently reported flow-like effects inside very high-multiplicity jets in pp collisions (96). This is unexpected and it would therefore be good if other experiments could

confirm the results. It would also be important to understand the partonic origin of these very high-multiplicity jets and to understand the new coordinate transformation involved in the measurement better.

There are two other directions that we think should be further explored in the case of flow in small systems. In AA collisions, one observes significant jet quenching meaning that jets lose energy as they propagate through the sQGP. As this is a final-state interaction and since final-state interactions are present in pp collisions, one would expect that jet quenching could also occur there. However, so far there are no indications of jet quenching in pp and pA collisions, see for example Refs. (97, 98). This could be due to the magnitude of jet quenching being too small or the statistical and systematic limits of available measurements too large, but it could also mean that there is no jet quenching in pp collisions. If this is the case then this must be an important part of understanding the origin of flow and strangeness enhancement in these systems and we therefore encourage theorists to explore this possibility.

The second direction is the possibility to use flow in a similar way as in AA collisions to learn about the microscopic event-by-event fluctuations in pp collisions, which could provide an alternative way to constrain the UE. There are for example indications that the flow is very sensitive to how the proton “geometry” is implemented in pA collisions (99). In a recent paper it was even suggested that the sign of the elliptic flow in pp collisions can be used to image the relevant degrees of freedom in the final state (100), i.e., that if v_2 is in fact negative then this would be an indication that the flow is not hydrodynamic but could be the result of Lund strings “shoving” each other or long-range partonic interactions. This raises a broader question related to flow in small systems: can we ignore the size of the fundamental degrees of freedom in these systems and neglect the precise interaction length as is done in hydrodynamic models? We hope for further phenomenological developments along these lines to provide new directions and to guide experimental investigations.

7. Conclusions and Outlook

At first sight, it may seem that a fundamental tension exists in soft QCD physics. On one hand, there is no direct evidence of saturation effects, and proton-proton collisions at 13 TeV are widely considered far from the Froissart-Martin bound. This suggests that partonic densities remain below the threshold for significant recombination effects. On the other hand, hydrodynamic models, which describe the evolution of dense and coherent systems, are frequently invoked to explain phenomena such as collective flow observed in multi-particle correlation measurements. This duality—where collisions are seen as both dilute enough to avoid saturation and dense enough to exhibit collective behavior—poses a significant challenge. Resolving this contradiction requires a deeper understanding of the interplay between partonic dynamics, saturation, and coherence in small systems.

The traditional pp paradigm that dominated soft QCD physics prior to the LHC was one that in some sense is derived from perturbative QCD. In particular for PYTHIA, the soft and hard physics was modeled similarly based on the idea of Jet Universality. With LHC, soft QCD physics has irreversibly changed as models have to add final-state interactions, such as color reconnection, between subcollisions and hadronization. One could add here that to some degree, even perturbative QCD has changed with the observation of charm and bottom baryons being enhanced over mesons with respect to $e^+e^- \rightarrow q\bar{q}$. Importantly, these effects were discovered at LHC but we re-find them in the data at lower beam energies.

The three main reasons for why these effects were discovered at LHC were the extended multiplicity reach of the LHC beam energies (as the effects grow with multiplicity), the larger focus on particle identification by in particular ALICE, and the new paradigm that AA collisions can be a reference for the search for QGP-like effects in pp collisions.

The breaking of Jet Universality raises new questions that could be ignored in the traditional, dilute pp paradigm. What are the relevant degrees of freedom after the subcollisions? How do they microscopically form/equilibrate and interact? It therefore appears that some aspects of the heavy ion paradigm could be applicable to pp collisions. Unfortunately, it seems that while the experimental questions of soft QCD in pp and AA collisions have merged, the theoretical/phenomenological approaches are living in parallel worlds. This is very unfortunate because the pp generator community have a huge expertise on the event-by-event fluctuations that are essential to model pp collisions, while the AA community have an expertise on these out-of-equilibrium processes that needs to be included when you have final-state interactions, see for example Ref. (101) for an overview. A stronger knowledge transfer and collaboration between these two groups could benefit the understanding of soft QCD at LHC tremendously. Furthermore, having AA-inspired phenomenology available in an open MC generator form that can be directly compared with the data (including biases due to, for example, multiplicity estimation) or used to devise tests to validate or falsify the proposed mechanism is urgently needed. To facilitate progress on this side, one should investigate if some of these mechanisms can be implemented as add-ons to existing pp generators.

On the experimental side there is a need to make more results available in a format that is easy to compare with pp generators, e.g., in RIVET. This would facilitate the tuning of models and also in general ensure the best apples-to-apples comparison with data. Tools have been developed to facilitate the new QGP-like analyses in RIVET (102), but there are still not many examples and it is therefore not always easy to implement the new analyses. A dedicated concentrated expert effort is needed to get this going.

Another important point to raise here is that the potential improvements of these efforts on the LHC discovery program needs to be investigated. Since most of the discovery program is focused on high p_T and most of the soft physics at low p_T it is not so obvious what can be gained. At the same time, this in some sense makes it even more important to carefully examine if this is indeed the case to not miss out on a big opportunity by the tremendous progress on our understanding of soft QCD at LHC.

Although dilute proton-proton (pp) collisions and dense heavy ion collisions may seem quite distinct, and one must be cautious when applying concepts from one to the other, we believe that addressing unresolved questions in soft QCD physics can benefit greatly from the exchange of ideas and analytical techniques between these areas. Such cross-fertilization is essential for improving the accuracy of models used to describe physics in unexplored energy ranges, such as those anticipated at future accelerator facilities.

Finally, we hope we have highlighted in this review that there is no reason to expect that the age of experimental exploration and digging for gold at the LHC is over.

*All that is gold does not glitter,
Not all those who wander are lost*
J.R.R. Tolkien

DISCLOSURE STATEMENT

If the authors have nothing to disclose, the following statement will be used: The authors are not aware of any affiliations, memberships, funding, or financial holdings that might be perceived as affecting the objectivity of this review.

ACKNOWLEDGMENTS

PC would like to thank the participants in the “QCD challenges from pp to AA collisions” International Workshop in Münster in September 2024 for inspiring presentations and discussions.

Support from the following research grants are gratefully acknowledged. Vetenskapsrådet contract 2021-05179 (PC). Knut and Alice Wallenberg foundation contract number 2017.0036 (PC).

LITERATURE CITED

1. Campbell JM, Huston JW, Stirling WJ. *Rept. Prog. Phys.* 70:89 (2007)
2. Grosse-Oetringhaus JF, Reygers K. *J. Phys. G* 37:083001 (2010)
3. Kittel W, De Wolf EA. Singapore: World Scientific Publishing (2005)
4. Collins PDB. vol. 4 of *Cambridge Monographs on Mathematical Physics*. Cambridge University Press (1977)
5. Ellis RK, Stirling WJ, Webber BR. vol. 8 of *Cambridge Monographs on Particle Physics, Nuclear Physics and Astronomy*. Cambridge University Press (1996)
6. Froissart M. *Phys. Rev.* 123:1053–1057 (1961)
7. Martin A. *AIP Conf. Proc.* 1105(1):258–261 (2009)
8. Kovchegov YV. *Phys. Rev. D* 60:034008 (1999)
9. Antchev G, et al. *Eur. Phys. J. C* 79(2):103 (2019)
10. Abramovsky VA, Gribov VN, Kancheli OV. *Yad. Fiz.* 18:595–616 (1973)
11. Koba Z, Nielsen HB, Olesen P. *Nucl. Phys. B* 40:317–334 (1972)
12. Blankenbecler R, Brodsky SJ, Gunion JF. *Phys. Lett. B* 42:461–465 (1972)
13. Kulchitsky Y, Tsiarshka P. *Eur. Phys. J. C* 82(5):462 (2022)
14. Chatrchyan S, et al. *JHEP* 08:086 (2011)
15. Buckley A, et al. *Phys. Rept.* 504:145–233 (2011)
16. Sjostrand T, van Zijl M. *Phys. Rev. D* 36:2019 (1987)
17. Bierlich C, et al. *SciPost Phys. Codeb.* 2022:8 (2022)
18. Bellm J, et al. *Eur. Phys. J. C* 76(4):196 (2016)
19. Pierog T, Karpenko I, Katzy JM, Yatsenko E, Werner K. *Phys. Rev. C* 92(3):034906 (2015)
20. Werner K. *Phys. Rev. C* 108(6):064903 (2023)
21. Karneyeu A, Mijovic L, Prestel S, Skands PZ. *Eur. Phys. J. C* 74:2714 (2014)
22. Hayrapetyan A, et al. *submitted to Phys. Rev. Lett.* (2024)
23. Sirunyan AM, et al. *Eur. Phys. J. C* 79(9):773 (2019)
24. Andronic A, Braun-Munzinger P, Redlich K, Stachel J. *Nature* 561(7723):321–330 (2018)
25. Chatrchyan S, et al. *Eur. Phys. J. C* 72:2164 (2012)
26. Ortiz Velasquez A, Christiansen P, Cuautle Flores E, Maldonado Cervantes I, Paić G. *Phys. Rev. Lett.* 111(4):042001 (2013)
27. Gelis F, Iancu E, Jalilian-Marian J, Venugopalan R. *Ann. Rev. Nucl. Part. Sci.* 60:463–489 (2010)
28. Bartalini P, Gaunt JR, eds. vol. 29 of *Advanced Series on Directions in High Energy Physics*. Singapore: World Scientific Publishing (2019)

29. Affolder T, et al. *Phys. Rev. D* 65:092002 (2002)
30. Buckley A, Hoeth H, Lacker H, Schulz H, von Seggern JE. *Eur. Phys. J. C* 65:331–357 (2010)
31. Bierlich C, et al. *SciPost Phys.* 8:026 (2020)
32. Sirunyan AM, et al. *Eur. Phys. J. C* 80(1):4 (2020)
33. ATLAS Collaboration. Tech. rep., CERN. ATL-PHYS-PUB-2014-021 (2014)
34. Tumasyan A, et al. *Eur. Phys. J. C* 83(7):587 (2023)
35. Aad G, et al. *Accepted by Eur. Phys. J. C* (2024)
36. Abelev B, et al. *Eur. Phys. J. C* 72:2124 (2012)
37. Aad G, et al. *Phys. Rev. D* 88(3):032004 (2013)
38. Acharya S, et al. *Eur. Phys. J. C* 79(10):857 (2019)
39. Chatrchyan S, et al. *JHEP* 04:072 (2013)
40. Sirunyan AM, et al. *Eur. Phys. J. C* 79(11):893 (2019)
41. Acharya S, et al. *JHEP* 08:086 (2022)
42. Aad G, et al. *JHEP* 07:019 (2012)
43. Aaboud M, et al. *Phys. Rev. C* 95(6):064914 (2017)
44. Alderweireldt S, Van Mechelen P. *arXiv:1203.2048 (hep-ph)* (2012)
45. Khachatryan V, et al. *JHEP* 09:091 (2010)
46. Adam J, et al. *Nature Phys.* 13:535–539 (2017)
47. Acharya S, et al. *Eur. Phys. J. C* 78(3):263 (2018)
48. Acharya S, et al. *Eur. Phys. J. C* 81(3):256 (2021)
49. d’Enterria D, Eskola KJ, Helenius I, Paukkunen H. *Nucl. Phys. B* 883:615–628 (2014)
50. Borsari I, de Florian D, Sassot R, Stratmann M. *Phys. Rev. D* 105(3):L031502 (2022)
51. Norrbin E, Sjostrand T. *Eur. Phys. J. C* 17:137–161 (2000)
52. Acharya S, et al. *Eur. Phys. J. C* 84(8):813 (2024)
53. Acharya S, et al. *Phys. Rev. C* 99(2):024906 (2019)
54. Fries RJ, Muller B, Nonaka C, Bass SA. *Phys. Rev. Lett.* 90:202303 (2003)
55. Acharya S, et al. *Phys. Rev. C* 107(6):064901 (2023)
56. Aaij R, et al. *Phys. Rev. Lett.* 132(8):081901 (2024)
57. Acharya S, et al. *JHEP* 07:136 (2023)
58. Acharya S, et al. *JHEP* 09:204 (2024)
59. Acharya S, et al. *JHEP* 05:184 (2024)
60. Christiansen JR, Skands PZ. *JHEP* 08:003 (2015)
61. Bierlich C, Gustafson G, Lönnblad L, Tarasov A. *JHEP* 03:148 (2015)
62. Acharya S, et al. *Eur. Phys. J. C* 80(8):693 (2020)
63. Gieseke S, Kirchgaeßer P, Plätzer S. *Eur. Phys. J. C* 78(2):99 (2018)
64. Werner K. *Phys. Rev. C* 109(1):014910 (2024)
65. Vislavicius V, Kalweit A. *arXiv:1610.03001 (nucl-ex)* (2016)
66. Vovchenko V, Dönigus B, Stoecker H. *Phys. Rev. C* 100(5):054906 (2019)
67. Cleymans J, Lo PM, Redlich K, Sharma N. *Phys. Rev. C* 103(1):014904 (2021)
68. Acharya S, et al. *JHEP* 09:102 (2024)
69. Adam J, et al. *Eur. Phys. J. C* 77(8):569 (2017), [Erratum: *Eur.Phys.J.C* 79, 998 (2019)]
70. Heinz U, Snellings R. *Ann. Rev. Nucl. Part. Sci.* 63:123–151 (2013)
71. Nagle JL, Zajc WA. *Ann. Rev. Nucl. Part. Sci.* 68:211–235 (2018)
72. Grosse-Oetringhaus JF, Wiedemann UA. *submitted to Annual Review of Particle Physics* (2024)
73. Kovtun P, Son DT, Starinets AO. *Phys. Rev. Lett.* 94:111601 (2005)
74. Schenke B, Tribedy P, Venugopalan R. *Phys. Rev. Lett.* 108:252301 (2012)
75. Bernhard JE, Moreland JS, Bass SA, Liu J, Heinz U. *Phys. Rev. C* 94(2):024907 (2016)
76. Acharya S, et al. *Phys. Rev. Lett.* 123(14):142301 (2019)
77. Abelev B, et al. *Phys. Lett. B* 719:29–41 (2013)
78. Aad G, et al. *Phys. Rev. Lett.* 110(18):182302 (2013)

79. Jia J, Zhou M, Trzupek A. *Phys. Rev. C* 96(3):034906 (2017)
80. Dusling K, Mace M, Venugopalan R. *Phys. Rev. Lett.* 120(4):042002 (2018)
81. Aidala C, et al. *Nature Phys.* 15(3):214–220 (2019)
82. Schenke B, Schlichting S, Singh P. *Phys. Rev. D* 105(9):094023 (2022)
83. Acharya S, et al. *Phys. Rev. Lett.* 132(17):172302 (2024)
84. Badea A, Baty A, Chang P, Innocenti GM, Maggi M, et al. *Phys. Rev. Lett.* 123(21):212002 (2019)
85. Chen YC, et al. *Phys. Lett. B* 856:138957 (2024)
86. Aad G, et al. *Phys. Rev. C* 104(1):014903 (2021)
87. Tumasyan A, et al. *Phys. Lett. B* 844:137905 (2023)
88. Abt I, et al. *JHEP* 04:070 (2020)
89. Abt I, et al. *JHEP* 12:102 (2021)
90. H1 Collaboration. Tech. rep., DESY. H1prelim-20-033 (2020)
91. Strickland M. *International Journal of Modern Physics E* (2024)
92. Kurkela A, Mazeliauskas A. *Phys. Rev. Lett.* 122:142301 (2019)
93. Ambrus VE, Schlichting S, Werthmann C. *Phys. Rev. Lett.* 130(15):152301 (2023)
94. Kurkela A, Wiedemann UA, Wu B. *Phys. Lett. B* 783:274–279 (2018)
95. Kurkela A, Mazeliauskas A, Törnkvist R. *JHEP* 11:216 (2021)
96. Hayrapetyan A, et al. *Phys. Rev. Lett.* 133(14):142301 (2024)
97. Acharya S, et al. *JHEP* 05:229 (2024)
98. Aad G, et al. *Phys. Rev. Lett.* 131(7):072301 (2023)
99. Mäntysaari H, Schenke B, Shen C, Tribedy P. *Phys. Lett. B* 772:681–686 (2017)
100. Bierlich C, Christiansen P, Gustafson G, Lönnblad L, Törnkvist R, Zapp K. *arXiv:2409.16093 (hep-ph)* (2024)
101. Berges J, Heller MP, Mazeliauskas A, Venugopalan R. *Rev. Mod. Phys.* 93(3):035003 (2021)
102. Bierlich C, et al. *Eur. Phys. J. C* 80(5):485 (2020)